7-14-2023

What Is a Polygonal Impact Crater? A Proposed Framework Toward Quantifying Crater Shapes

Stuart J. Robbins

Jamie D. Riggs

Earth and Space Science

RESEARCH ARTICLE
10.1029/2023EA002863

What Is a Polygonal Impact Crater? A Proposed Framework Toward Quantifying Crater Shapes

Stuart J. Robbins[1] **and Jamie D. Riggs**[2]

[1]Southwest Research Institute, Boulder, CO, USA, [2]Thomas Jefferson University, Philadelphia, PA, USA

Key Points:

- An objective algorithm to fit polygons to impact craters, with and without curved sides, is presented
- The code concludes that Fejokoo crater (Ceres) is best represented by a straight-sided hexagon, matching previous manual work
- Absence of strong differences between Monte Carlo fits to the same crater is interpreted as a lack of strong structural control

Correspondence to:
S. J. Robbins,
stuart@boulder.swri.edu

Citation:
Robbins, S. J., & Riggs, J. D. (2023). What is a polygonal impact crater? A proposed framework toward quantifying crater shapes. *Earth and Space Science*, *10*, e2023EA002863. https://doi.org/10.1029/2023EA002863

Received 30 JAN 2023
Accepted 30 APR 2023

Author Contributions:
Conceptualization: Stuart J. Robbins
Data curation: Stuart J. Robbins
Formal analysis: Stuart J. Robbins, Jamie D. Riggs
Funding acquisition: Stuart J. Robbins
Investigation: Stuart J. Robbins, Jamie D. Riggs
Methodology: Stuart J. Robbins, Jamie D. Riggs
Project Administration: Stuart J. Robbins
Resources: Stuart J. Robbins
Software: Stuart J. Robbins, Jamie D. Riggs
Supervision: Stuart J. Robbins
Validation: Stuart J. Robbins, Jamie D. Riggs
Visualization: Stuart J. Robbins
Writing – original draft: Stuart J. Robbins

Abstract Impact craters are used for a wide array of investigations of planetary surfaces. A crater form that is somewhat rare, forming only ~10% of impact craters, is the polygonal impact crater (or PIC). These craters have been visually, manually identified as having at least two rim segments that are best represented as straight lines. Such straight lines or edges are most often used to infer details about the subsurface crust where faults control the structure of the crater cavity as it formed. The PIC literature is scant, but almost exclusively these craters are identified manually, and the potentially straight edges are classified and measured manually. The reliance on human subjectivity in both the identification and measurement motivated us to design a more objective algorithm to fit the crater rim shape, measure any straight edges, and measure joint angles between straight edges. The developed code uses a Monte Carlo approach from a user-input number of edges to first find a reasonable shape from purely random possible shapes; it then uses an iterative Monte Carlo approach to improve the shape until a minimum difference between the shape and rim trace is found. It returns the result in a concise, parameterized form. This code is presented as a first step because, while we experimented with several different metrics, we could not find one that could consistently, objectively return an answer that stated which shape for a given crater was the best; this objective metric is an area for future improvement.

Plain Language Summary Features on planetary bodies are often parameterized in databases, meaning that they are concisely represented in some way. This conciseness requires finding some method to summarize the information about the features. For impact craters, this is most often done by reducing a crater to three simple numbers: The latitude of the center, longitude of the center, and diameter of the crater. However, information about the shape of the crater's rim is lost when one assumes it is a simple circle. Some research applications investigate crater rims as polygons with two or more straight sides. Measurement of those sides is often subjective and almost always done manually. In this work, we have written an objective computer algorithm to try to determine how many sides represent the crater rim. This code can include straight and curved sides, and it can return the answer in a compact way for input into a database. This code is presented as a first step toward making these measurements objectively because it presently has no method to objectively state if one shape is better than another, instead still relying on the human analyst.

1. Introduction

Planetary features have long been parameterized to simplify them for cataloging and analysis. Parameterization necessarily removes information about the feature in order to summarize it, trying to reduce the feature to its most important components. The study of polygonal impact craters (PICs) has a diverse—if small—literature set with different researchers discussing PICs across various planetary bodies, from Mercury through the asteroid belt, giant planet satellites, and out to Charon. This type of crater is investigated because it can lead to information about otherwise hidden subsurface fracturing or porosity that are significant enough to control the expanding shock that emanates from impact (see discussions in Öhman, 2009, and Beddingfield et al., 2016, for more detailed implications). A key, long-standing method to study these features is to parameterize them by classifying the number of sides, the bearing or azimuth of those sides, and angles they make when next to each other. These data are most often used to make various conclusions about PIC formation, usually based on observed or inferred faults.

Unfortunately, there is no objective standard for what is considered to be an edge, how to measure the angle of that edge, nor what counts as a joint (where edges meet), and hence there is an uncomfortable amount of subjectivity in existing studies that can make them hard to independently replicate or test. Indeed, to the eye, some basic results are repeatable, such that there might be broad agreement that an impact structure has approximately six

Writing – review & editing: Stuart J. Robbins, Jamie D. Riggs

straight edges. However, this is usually limited to strong or "obvious" cases, which raises the concern about what makes something "obvious:" Something "obvious" to one researcher might not be "obvious" to the next, much like a professor describing how it is obvious that $e^{i\pi} = -1$ while confused students sit quietly taking notes. Even if the number of straight edges might be widely agreed upon, the direction of those edges have no exact definition, and when features are no longer plainly obvious, interpretation can vary significantly. This propagates to uncertainty in any type of conclusion that might be made about the features, including their origin, modification history, and existence of underlying structure beneath a planetary body's surface that might have guided their formation. While some authors have incorporated more objective and quantitative definitions and tests, they are not implemented beyond those authors (see the next section for further discussion).

This work presents effort toward the development of a new, objective method to determine the polygonality of impact craters based on a Monte Carlo approach of testing different shapes and calculating how well they approximate the crater rim. The primary goal of this algorithm is to take the human subjectivity out of the parameterization process so that objectivity—and hence replicability—can exist. In Section 2 of this work, past studies on PICs are summarized. Section 3 describes how the algorithm works, and Section 4 has numerous type examples from the inner solar system. The discussion in Section 5 focuses on implications and potential future code or method improvements. The code is written in Python and is freely available on two platforms (see Data Availability Statement), and it includes a user manual as a PDF document on both platforms.

2. Past Studies on Polygonal Impact Craters

Published literature exists that identify PICs from Mercury through Charon, and while PICs have been observed for over a century, relatively little literature about them exists. There was a push in the second half of the twentieth century based on new spacecraft data of planetary surfaces throughout the solar system, while modern work in the last ∼15 years has been limited to just a few researchers presenting mostly in conference abstract form. This small resurgence might be due in part to the much better data of Saturn's satellites returned by *Cassini* starting in 2004; the *MESSENGER* spacecraft returning the first new Mercury images in decades starting in 2008; and the orbital insertion of *Dawn* at Vesta in 2011, and its subsequent orbital insertion at Ceres in 2015. Saturn's moons, Ceres, Mars, and to a lesser extent Vesta provide the vast majority of visually obvious, convincing PICs. The review presented in this section is meant to paint a picture of the relatively little attention to PICs that has been made in the modern literature—especially the peer-reviewed literature—and that the majority of work uses PICs to explore potential underlying faults and fractures that are not visible. For a much more complete review of pre-2010 work, see the doctoral dissertation by Öhman (2009).

Working out from the Sun, Weihs et al. (2015) is the only modern peer-reviewed work to examine PICs on Mercury, though a few earlier works exist that describe them (Dzurisin, 1978; Melosh & Dzurisin, 1978). Weihs et al. (2015) examined 291 named craters with diameters $D > 12$ km, globally, finding that 33 were polygonal, which was within the 10%–15% expected range from other bodies based on summaries by Öhman (2009). For their work, the definition of "polygonal" was "at least two straight rim segments." However, what that means in practice is not clear given that any rim is straight if examined over a small enough length scale, or it is straight given a large enough tolerance for any deviations; they did not define how polygonality was measured beyond the above statement. One example PIC they describe is the crater Mahler, which is discussed further in this work's Section 4.1.

Moving outwards from the Sun to Venus, Herrick (1997) database includes 4 craters classified as polygonal, while conference abstracts by Öhman et al. (2007) and Aittola et al. (2008), and the peer-reviewed paper by Aittola et al. (2007) describe some Venusian PICs; their example of Behn is discussed in Section 4.2. They visually examined craters $D > 12$ km for any apparent straight rim segments and identified 131 craters that "clearly display at least two straight rim segments and a clearly discernible angle between them." Using that qualitatively defined quantitative definition, they found that 13% of Venus' craters are PICs. Again, no further definition of polygonality nor method of measuring sides and angles was described, nor was there a description of how the extreme emission angle of left- or right-looking radar might affect the appearance of straightness or curvilinearity.

The type example on Earth is Meteor Crater in Arizona, USA; this is discussed further in Section 4.3. Earth's moon has received little PIC attention in the modern literature, despite the plethora of data for that body, which

we interpret as it having fairly little consensus or identification of a sizable PIC population. The only instance we could find was in a general review paper (Öhman et al., 2010) based on a dissertation (Öhman, 2009), which compared the population of lunar PICs to those on other bodies, and other than that discussed pre-modern (*Apollo*-era and earlier) studies. In their work, the definition of "polygonal" was: "based on careful visual inspection of the imagery, the crater was required to have two adjacent straight rim segments to be classified as polygonal." Again, no further explanation was given, which we infer to mean that these were subjectively measured as in most studies.

Mars has received more attention, primarily from Öhman and colleagues (e.g., Öhman, 2009; Öhman et al., 2005, 2008). Their work looked at PICs within the megameter-sized Hellas and Argyre craters and used those PICs to infer tectonic stress patterns. They reported 10%–20% of impact craters were polygonal. Conference abstracts by Watters and Zuber (2007, 2009) also looked at small PICs (generally sub-kilometer) and described their approach almost as much as their results: They used "machine vision technologies" to automate some of the measurements, removing a significant amount of human subjectivity. Öhman et al. (2010) note that this was the only study to-date that had such objectivity, except for Eppler et al. (1977, 1983) who used Fourier shape analysis methods (something we, also, examined; see Section 5).

With *Dawn* at Ceres in 2015, several different authors published conference abstracts examining Cere's plentiful PIC population: Otto et al. (2015, 2016) looked at latitudinal distribution and numbers of sides; Neidhart et al. (2017) looked at Ceres in context of other bodies; Zeilnhofer and Barlow (2018) discussed joint angles, sides, and relationship with fractures. Peer-reviewed work by Gou et al. (2018) included 276 PICs in their database, and Krohn et al. (2019) included a PIC discussion in a report about Cerean asymmetric craters that focused on broader implications about global fractures. None of the preceding referenced works described any metric for determining polygonality. The Zeilnhofer & Barlow work formed part of Zeilnhofer's doctoral dissertation (Zeilnhofer, 2020) and two papers the next year (Zeilnhofer & Barlow, 2021a, 2021b). Out of all these published works, only Zeilnhofer and Barlow (2021b) described how polygons were measured: sides were defined as whether an angle is measurable to join them; if so, then lengths and sides were drawn by hand, and azimuths and joint angles then measured in computer software.

In the outer solar system, the literature is similarly sparse, though PICs on outer solar system surfaces appear to be more prevalent or at least less ambiguous. The Galilean satellites all have PICs, while the Saturnian satellites, due almost certainly to the larger data volume, have better studied PICs. The very recent conference abstract by Baby et al. (2023) addresses PICs on Ganymede, describing PICs as having 1–9 sides (as opposed to $\geq$2 by most work) and that they appear on all terrain types, but no description of objective measurement was presented. The conference abstract of Neidhart et al. (2017) discusses a diameter comparison and number of straight rim segments comparison among several bodies, including Rhea, Dione, and Tethys. Beddingfield et al. (2016) is the only modern (*Cassini*-era) peer-reviewed paper that investigated PIC in the Saturnian system. Their work looked at PIC populations and rim segment azimuths in Dione's wispy and non-wispy terrains, and they used those PICs to infer subtle (unseen) fractures that were consistent with satellite despinning and volume expansion.

Beddingfield and Cartwright (2020) moved further out by examining Uranus' moon Miranda, analyzing 14 PICs, the trending directions of their sides, and used them to infer information about hidden tectonism below Miranda's surface. In conference abstract form, Beddingfield et al. (2020) reported on preliminary work identifying PICs on Charon, again with implications about the tectonic field in Charon's crust. Beddingfield's various papers and conference abstracts on the subject are the most objective that we could find in the modern literature, wherein they perform several different statistical tests on crater rim traces that the craters must pass before concluding they are a PIC. With that in mind, we found practically no discussion about projection effects, and how measuring geodetics on different map projections without properly accounting for those projections can affect the angles measured. This is something our code addresses.

3. An Approach to Objectively Parameterizing Polygonal Impact Craters

3.1. Setup of the Problem

The first goal in developing this objective computer algorithm was to take what the human eye and brain do naturally and objectively codify it by asking the question: What is the best, simple shape that can represent this crater? In this context, a "simple shape" could mean a circle, ellipse, or some sort of irregular polygon that may

or may not incorporate some components that are curved. When examining an impact crater, the brain tends to "know" when it sees straight sides or angles in the edges; hence, "we know it when we see it" is a phrase that comes to mind. However, in-between cases are subjective, and what is "obviously" a PIC to one person might not be to another. Similarly, for real planetary features that are not perfect polygons, the brain must make decisions about what to include in an edge, not include in an edge (i.e., where to place the joint), and how to accurately draw that edge.

After parameterizing a feature, the second goal in developing this code was to represent the feature in as compact a form as possible such that one can resurrect the pertinent information accurately and easily. For example, for the vast majority of impact crater studies, craters are reduced to three parameters: latitude, longitude, and diameter (or sometimes radius). For polygonal craters, the interest is in the edges, where those edges meet, whether any edge is an arc, and then what the radius and end points of that arc are, so the problem is not as compact. For a given N-sided polygon that has N vertices, the problem can be reduced to $3 \cdot N+3$ parameters: for each n_i vertex, the latitude and longitude must be included, and a flag for whether it is linked to the next vertex with a straight line or an arc; additionally, two parameters for the central latitude and longitude of all arcs and their shared radius are needed. All bearings and joint angles can be computed *post facto* from that information.

3.2. Data Required for the Algorithm

We have written the algorithm to accept a simple list of latitude-longitude pairs in decimal degrees that represent a crater rim trace. How those were measured is completely up to the user's discretion, but as with most impact crater studies, there are some components that must be kept in mind.

One component is the resolution of the impact crater—how many pixels across it must be to reasonably resolve its shape and to trace it for input to this algorithm. Mathematically, there must be at least as many points in a rim trace as parameters to be fit (e.g., a circle must have at least three points to define it, and an ellipse must have at least five). Realistically, the crater should be at least >10 pixels across to reliably measure it (Robbins et al., 2014), and if that minimum size, it is recommended that the user trace the rim with 1 vertex per pixel fidelity to provide as detailed a rim trace as possible. Beyond that, we can only recommend that the more pixels one has, the better resolved the feature is, and so the more likely the code's output is to represent reality. Similarly, we also recommend that this only be done with reasonably well preserved craters, even though in our example section we include one highly degraded crater. If a crater is not well preserved, the rim can be poorly defined, leading to significantly more uncertainty which cannot be easily quantified.

Similarly, the data set one uses to identify the crater could potentially affect results. Topography, while more rare in our planetary data archives, tends to be better for identifying impact crater shapes because one can recognize the rim crest independent of sun angles. With images instead of topography, rims tend to disappear when parallel to the incident sun, which means that when one traces that region of the rim, one could artificially straighten the rim in those locations. It is difficult to get past this, but typically those regions are relatively small components of the overall crater rim. It is also preferable for any data set used to be close to nadir; foreshortening caused by non-zero emission angles, such as side-scan radar, can affect angles and create or enhance an apparent straightness of an edge.

Finally, the code assumes a rim trace is complete, that it does not have any significant gaps. It will treat gaps as straight edges, which one could remove in post-processing.

3.3. Description of the Algorithm

The algorithm begins by processing the data into a form that can be accurately analyzed from a geodetic perspective. This work is based on code developed for fitting circles and ellipses (Robbins, 2019; Robbins & Hynek, 2012) that begins by reading an ASCII file of a crater rim trace in units of decimal degrees. The code converts the rim trace into kilometers from the rim's centroid using Great Circles distances and bearings that assume a biaxial ellipsoid body (Vincenty, 1975). For self-similarity and boundary consistency across different-sized craters for this polygonal analysis, a linear scaling is applied to normalize the crater to fit inside of a box with an area ≈ 1, centered at the origin (0, 0). It applies the scaling and projection in reverse to all final parameters.

The code then attempts to fit a closed shape. It will fit a circle for reference, and after that it will fit an n-gon where $n \geq 3$. There is no restriction for the polygon to be regular (meaning that it is not required for all sides and

angles to be equal), and it can also allow one or more sides to be arcs. The shape must be closed, since crater rims are closed. The fundamental shape optimization behind the code is that it seeks to minimize the area difference between the rim trace and the fitted polygon. For example, one might have a perfect square as a rim trace, and the code initially guesses a square that is offset to the left. The shape enclosed by the rim trace is subtracted from the shape enclosed by the polygon fit, and the area of the remainder is calculated. If the code shifts the fit to the left, the area subtracted increases, so the code would know that is not a better fit and throw it out. If the code shifts the fit to the right, the area subtracted decreases, so it would know that is an improvement and the shift should be retained.

Using that concept, the code uses a Monte Carlo approach in two stages. The code can test N-dimensional polygons with the possibility of $\leq \lfloor N \div 2 \rfloor$ of the sides being an arc (e.g., if $N = 3$, then 0 or 1 side could be an arc). This means that the next two paragraphs are repeated as many times as different-n-gons are tested. It also has the ability to perform the fits multiple times with random seeds to test for repeatability (described later). Reasonable limits need to be placed on N to avoid ad infinitum compute time and over-fitting, also discussed later.

The first Monte Carlo stage is to randomly guess where the N vertex points will be. Random draws from the rim trace, plus some random noise, are taken, with three constraints. In versions where $\geq$1 side can be an arc, the side(s) to be an arc is/are chosen randomly. However, once one is set, any additional side(s) that is/are arcs must be separated by a straight side; otherwise, the fit would effectively be an N–1 shape. A second, empirical requirement is placed where the angle connecting any two adjacent vertices with the shape's center must be $\geq(360° \div N)\div 3$ to avoid seeding cases of two nearly adjacent vertex points. The third constraint is that the test shape must be convex, meaning no joint can be $\geq$180° measured inside the shape. This stage is run m_1 times, and the polygon that minimizes the area difference is saved. $m_1 \sim 500$ is often enough for well-defined shapes, but inclusion of arcs instead of all straight edges makes the problem more computationally difficult. The more arcs and sides included, the more subtle differences are possible, so $m_1 = 1{,}000 \cdot N$ by default (additionally, the more arcs and sides included, the more circular the fit becomes, raising the issue of over-fitting; see Section 5).

The second Monte Carlo stage takes the best polygon from the first stage and jitters the points with Gaussian noise, determining if there is an improvement. If there is, that new shape is saved as the best, and the next iteration proceeds from it. After a certain number of iterations, the Gaussian noise is decreased (commonly referred to as a "simmer"), so smaller changes are made as the algorithm settles on a solution. A purely random walk Monte Carlo approach is primarily employed, though it has been slightly optimized with a naïve Metropolis-Hastings implementation of a Markov chain Monte Carlo (Hastings, 1970), which takes the previous improvement (if the previous iteration was an improvement) and uses that as a slight offset in the next iteration's random walk. Using the perfect square example from before, the code would recognize that a slight shift to the right improved the fit, so instead of the next iteration having purely random noise applied, it is random noise with another slight offset toward the right. The randomness is also constrained in that the solution must be concave (no interior angles $\geq$180°), so if the jitter would make the shape convex, it is rejected. The angle separation of vertices is not enforced at this stage. This second stage is run m_2 times, and $m_2 \sim 10{,}000$ converges well, though tests in the next sections were run to 15,000 iterations to check for convergence.

We explored several different methods to return an objective measure for which of the minimized final polygons are best, for example, if the best pentagon is a better fit than the best octagon with one side as an arc. Such a metric must return a result that takes into account that the more free parameters (sides) one adds, the better the fit will be; in other words, the metric must penalize the goodness of the fit based on the number of degrees-of-freedom (DOF). As a very simple thought experiment, while a 100-sided polygon might fit a crater rim very well, a circle might fit it almost as well; a circle has 3 parameters, while a 100-sided polygon has >200, so the circle would be the preferred fit. We unfortunately were unsuccessful in finding or developing an objective metric that worked well in all cases. Until such a metric can be found, this code should be treated as a more probabilistic approach where the researcher can use it to inform their own decision (demonstrated in Section 4).

From the code's output parameters, it is relatively trivial to reconstruct azimuths of any sides that are straight lines (as opposed to any that are arcs). While the simplest method to calculate azimuth would be basic Cartesian trigonometry (e.g., $\alpha = \tan^{-1}((\varphi_{i-1} - \varphi_i)\div(\lambda_{i-1} - \lambda_i))$, where φ is latitude and λ is longitude), it is recommended that one uses the formulae that factor in proper geometry on an ellipsoid (Vincenty, 1975), which this code does.

Finally, this code does not output any uncertainty metric. It does output the normalized area difference between the shape fit and the rim trace which can be used as some metric of residual uncertainties, but we think that the

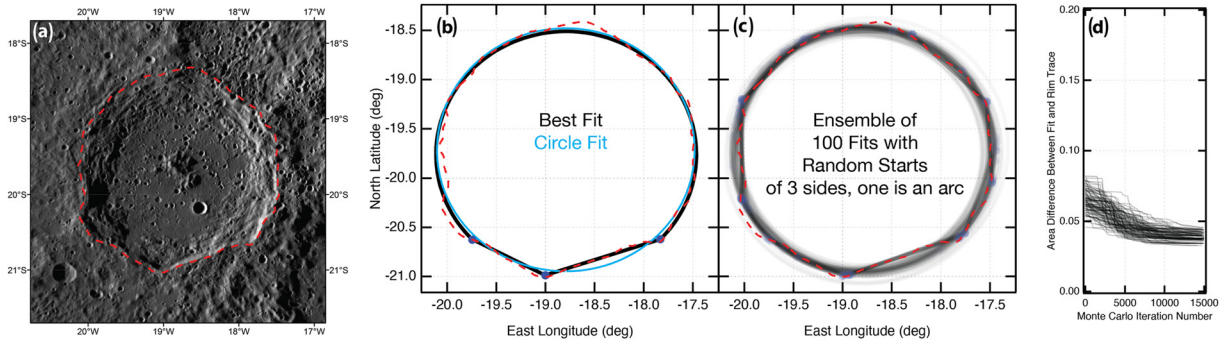

Figure 1. In these plots, the panel with the satellite data is in a local projection system, while all plots with rim fits are in equirectangular and so may show latitude compression effects. (a) Mahler crater (Mercury) example with rim trace (on the 166 m/pix MDIS mosaic). (b) Best fit from this code to Weihs et al. (2015) shape, along with a best-fit circle for comparison and the rim trace overlaid. (c) Example 100 runs of that shape (a triangle with one side as an arc) with reduced opacity, so more common solutions are darker. The shape is black (or gray) while the vertex points are shown in blue. (d) Area minimization of the 100 runs showing that the same minimum was not always obtained.

various versions of the final shape returned—along with the parameters for each from the previous paragraph—represent a good way to understand the uncertainty in the fit.

4. Examples

4.1. Example: Mercury's Mahler—An Ice Cream Cone Shape

Mercury's Mahler crater (Figure 1) is an example of a crater proposed to have a single joint at the apex of two straight lines which are then connected by an arc. Mahler is the type example PIC in Weihs et al. (2015). We traced Mahler using 556 rim vertex points on the 166 m/pix Mercury Dual Imaging System (MDIS) mosaic and constrained our code to find three sides where one was an arc. The Mahler experiment also set our angle requirement on how close the randomly selected points could be: Initially, it was $(360° \div N) \div 2$, but the approximate vertices in Weihs et al. (2015) are ∼42° from each other, meaning we prevented the code from finding them as a possible solution.

For this and other type examples throughout this section, the code was run 100 times for each discussed geometry and results analyzed in two ways. The first method, shown in several figures, is a visual examination of the various minimized rim geometries with significant transparency applied, which allows common solutions to appear more obvious due to overlapping opacity (e.g., Figure 1c). The second method is to look at the convergence area differences between the minimized shape and the crater rim, also shown in several figures (e.g., Figure 1d).

In relatively few solutions did the code lock onto the shape proposed by Weihs et al. (2015). In general, the code randomly locked onto different areas of relatively straight rim segments, slightly preferring the northwest and southwest. When forced to arrive at their solution, it was a true minimum in the area difference, but only extremely slightly (0.0344 vs. other minima that were as low as 0.0345). This is in comparison to a circle that has an area difference of 0.0434. Those values, coupled with examination of Figure 1a–1c, indicate that Mahler really is probably better modeled as a circle. It is possible that the East-West lighting geometry, coupled with their vertex at the south point, could be why the brain interprets this as a more polygonal crater than it actually is.

For a sanity check, and since this is the first example discussed, a triangle with no arcs was also fit (not shown). The area difference was 0.2443, though the fit converged 100% of the time to the exact same triangle. Therefore, just because it converges the same way every time, that does not mean it is a good model for the crater shape.

Finally, for the sake of comparison, when the code is forced to converge to the Weihs et al. solution via very precisely seeding it with that shape, the optimized joint at the southern point of the crater is 133.1°, close to the 125° published by Weihs et al. (2015), and practically identical given that most authors construct rose diagrams of joints and side bearings in intervals of 10° or 15°. Also, our calculation incorporates Great Circle bearings, which will lead to slightly different results even with Mahler's relatively equatorial latitude of ≈ – 20°.

4.2. Example: Venus' Behn—A Pentagon With an Arc

Behn (Figure 2) is a named type example of a PIC described in Öhman et al. (2007) and Aitolla et al. (2007, 2008). The former described it as having at least two straight sides, while the latter drew four segments that were joined

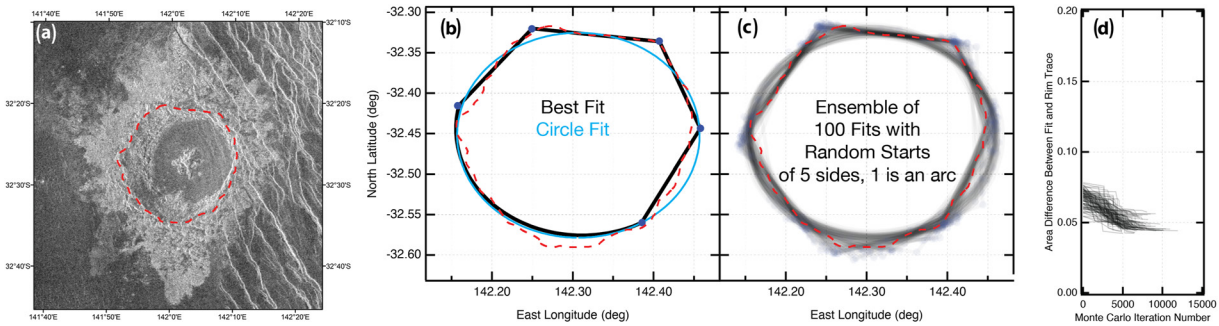

Figure 2. Example of Behn crater (Venus; 75 m/pix left-looking *Magellan* radar) following the same panel layout as in Figure 1. Panel (d) shows that, with a large arc and several vertex points, the fit will often converge before the maximum number of runs, though it does not always converge to an absolute minimum.

by approximately the angles of a regular hexagon, and they left the southwest portion of the crater unsketched. They listed the trending directions of the different rim segments as 34° (northwest segment), 96° (north segment), 153° (northeast segment), and 28° (southeast segment), and estimated a ±7.5° uncertainty (they considered any angles within 15° to have parallel sides).

We traced the rim using 340 vertex points on the 75 m/pix left-looking *Magellan* radar mosaics. It should be noted that these data are not orthorectified, as evidenced by the extreme enhancement of the western crater wall but complete masking of the eastern; this could affect polygonality due to foreshortening, and it could affect any angles calculated. The code was able to find the above-reported shape, and the bearings found were 37°, 97°, 158°, and 206° (or, 26° modulo 180°). These are within the estimated Aitolla et al. (2007) ±7.5° uncertainty. However, other runs found different versions of a polygon made of five sides with one side being an arc, and the area difference between the fit and the polygon indicated these were only slightly worse. Figure 2 shows that while there is a small preference for the segments identified by Aitolla et al. (2007), they are again not strong minima in various incarnations of the pentagonal fit with one arc, as in they are not strong drivers for an optimized shape.

The area difference between a circle and Behn's rim is 0.0756, while the optimized pentagon with one arc is 0.0423. This is a substantial improvement, but at the cost of significantly more fit parameters, and with a large asterisk about the oblique imaging.

4.3. Example: Earth's Meteor Crater—A Quadrilateral, or Octagon With Four Arcs

Meteor Crater is Earth's best-preserved kilometer-scale impact crater, near Winslow, AZ, USA. The structure has long been recognized to have four approximately straight edges, which are known to be controlled by nearby faults, so we can see how the code handled the structure. The focus of this test was to look at how the code discriminated between a circle fit, a four-sided polygon fit, and an eight-sided polygon with four curved edges. For tracing, we used a 50M-point topography cloud that had roughly 1 m spacing.

The results are shown in Figure 3. Based on area differences, a circle fit is a better fit than a quadrilateral, though the quadrilateral is able to capture the sides (bearings approximately 74.7°, 163.9°, 251.3°, and 342.3°). The best fit, however, is the octagon with alternating arcs (with straight sides of bearings 77.9°, 166.7°, 256.0°, 345.2°). The sides and their bearings are slightly different between the quadrilateral and octagon. The reason is that the code's sole method of determining a good fit is to minimize the area difference between the fit and the rim trace. Because the quadrilateral has sharp corners, the code must shift the quadrilateral's corners to minimize that difference between the quadrilateral shape both outside and inside the rim trace. Adjusting one corner shifts two edges, so that tradeoff affects the bearing/azimuth of the sides away from what one might think to be a better solution.

Figure 3 also demonstrates that the code was not always able to lock onto the most optimized octagonal shape. This is because there are so many free parameters that, despite the octagon with four arcs being the best solution, it is still not always simple for the code to find it. This is an area for code improvement and why we recommend running the code multiple times with the same *N* sides to see if it converges to the same (or very similar) shape each time.

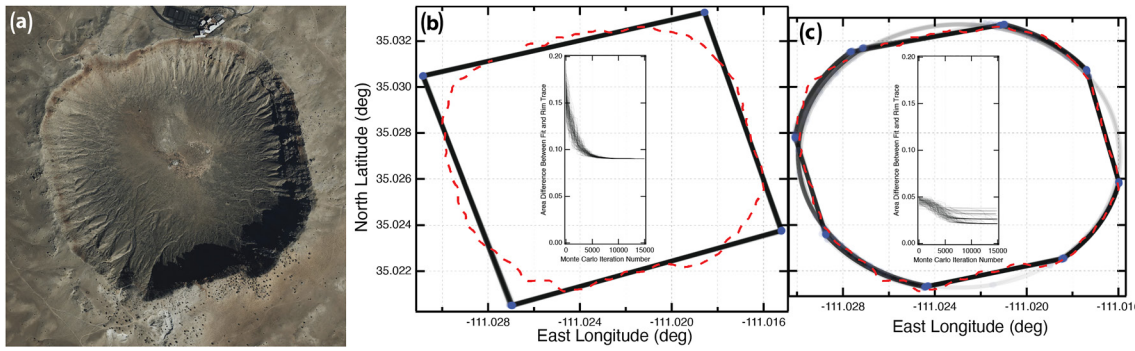

Figure 3. Example of Meteor Crater (Earth; image is from satellite data via Digital Globe) following the same panel layout as Figure 1, but convergence data are inside of the final fitted shapes. Panel (b) is a quadrilateral fit, while (c) is an octagon where four sides are arcs.

4.4. Example: Moon's Copernicus—A Polygonal Crater?

Copernicus has sometimes been identified as a polygonal crater (e.g., Öhman et al., 2005). However, subjectively looking at the impact, one might find it difficult to decide whether there are straight edges or simply concave ripples due to the scalloped nature of the rim, which is common for complex craters ($D \gtrsim 15$ km on the Moon; Pike, 1980). We traced the rim with 2,952 vertex points using the 100 m/pix Lunar Reconnaissance Orbiter Camera Wide-Angle Camera (LROC-WAC) mosaic, and a large suite of 19 possible shapes ($N = 4$–8, with 0–$\lfloor(N \div 2)\rfloor$ arcs) were run, 100 times each, in addition to a circle fit. The matrix of results is shown in Figure 4.

Interestingly, most solutions that included arcs converged on there being an arc across the northern rim, which is in contrast with past work that indicated the northern rim was the most distinct polygonal side (keying in on the cusp near the 11:00 position). Most higher-order solutions tended to converge to lower-order versions (two or more vertices almost on top of each other), and most $N \geq 6$ with ≥2 arcs converged almost to a circle (minimizing the lengths of the straight sides). Also, most higher-order solutions were non-unique: Running multiple times converged upon completely different solutions. The opacity of the straight lines along the southeast and south-southeast rim is more than elsewhere, including the arcs over those areas, indicating a small preference for straight edges in those regions.

There is also the curious case of the hexagon fit. Unlike Mahler or Meteor Crater where the triangle and quadrilateral fits converged to the same result each time, respectively—despite neither being optimal shapes—the quadrilateral, pentagon, heptagon, and octagon fits to Copernicus failed to have any strong convergence to a single fit. The hexagon is a slight outlier, where the northern ~⅔ of the crater converged well to four distinct rim segments with relatively little difference between the runs, while the southern part had a large suite of possible locations and therefore angles for the southern vertex. Further, the two most common southern edges are different from the two mentioned above for when arcs were allowed and two strong southern straight segments emerged.

The issue then arises of how one should interpret these seemingly contradictory results. If one desired, one could certainly point to the above paragraph and state that there are four reasonably consistent sides in a hexagonal fit, there could be underlying lunar stress patterns that parallel them, and look for further evidence of them from other craters or geologic features. The same goes for the two possible southeastern edges noted two paragraphs earlier: In and of themselves, they are not strong evidence for underlying control of Copernicus' shape, but they are suggestive that further searches could be made. An alternative interpretation, and one that we cannot rule out in the absence of a good criterion that penalizes over-fitting to quantitatively suggest a best shape, is that the dizzying array of different solutions is indicative of a null hypothesis that Copernicus is best modeled as a circle, and the appearance of straight rim segments is an illusion.

4.5. Example: Ceres' Fejokoo—A Hexagon

Fejokoo crater (Figure 5) is one of the primary type examples of polygonal craters on Ceres—and at this point, probably in the Solar System. It is commonly reported as a hexagonal crater, and indeed, to the eye, it does appear to be hexagonal. However, one can see that the south and east components of the rim might pose problems to a computer algorithm. Specifically, the eastern rim appears to have two distinct edges, but the joint between them

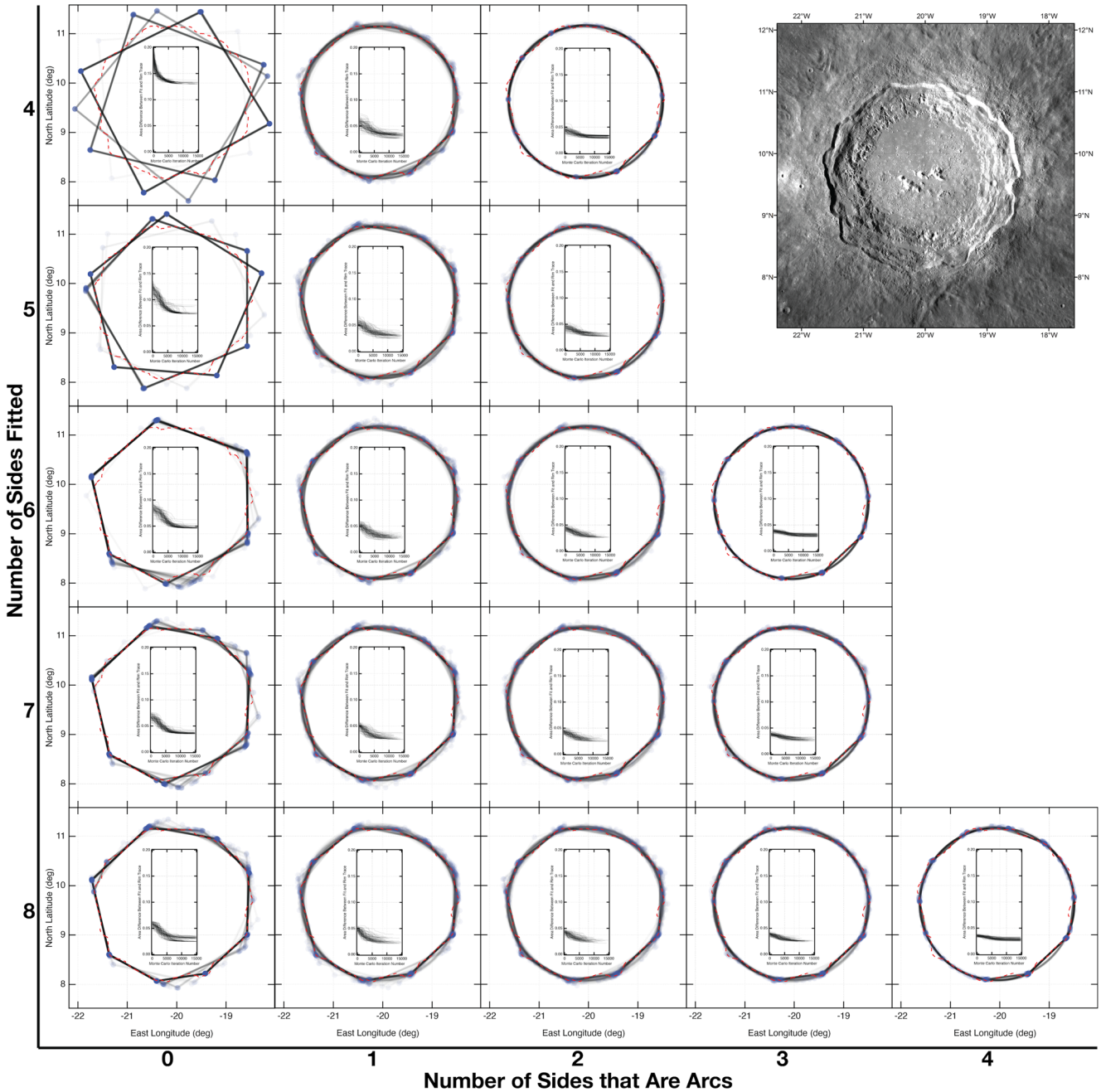

Figure 4. Example of Copernicus (Moon; 100 m/pix LROC-WAC mosaic), with a large parameter space of 100 runs each. The plots follow panels (c) with (d) inset from the Mahler and Behn examples, while the crater is in the upper-right for reference without the rim trace overlaid.

is smaller and more gradual than some of the variation seen within a single edge elsewhere on the crater rim. The southern component of the rim could be interpreted by eye as having one long edge with significant variation within it, or up to three straighter segments, each again with relatively small-angle joints. This analysis is independent of geologic context, where the shape of the south rim might be influenced by the superposed crater near it, and the geology of the eastern rim is likely heavily influenced by collapse. Regardless of geology, the code was applied to determine the optimum shape and see if it reproduced a hexagon or something else.

The crater is $D \approx 68$ km and is centered near 132°E, +29°N, and we traced its rim using 1,036 points on the 140 m/pix *Dawn* mosaic. The same suite of shapes as for Copernicus was run. In contrast with Mahler, Behn, and Copernicus, extremely consistent (and reassuring) results were obtained with Fejokoo. For shapes with no

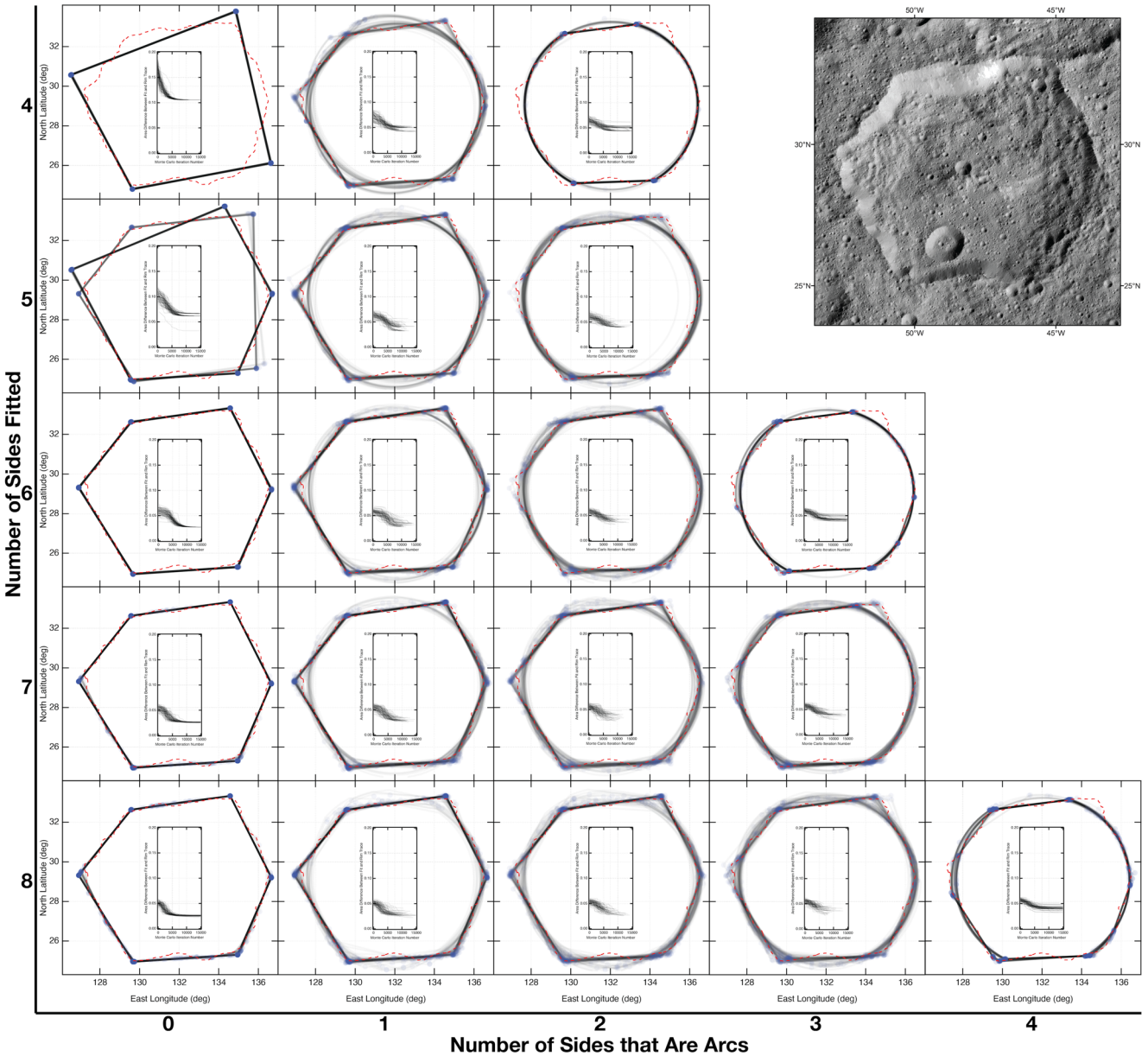

Figure 5. Same as Figure 4, except showing Fejokoo crater (Ceres; 140 m/pix *Dawn* mosaic).

arcs, the quadrilateral converged every time to a single shape, the pentagon to a suite of mainly two shapes, and hexagon to the same shape each time. Interestingly, the heptagon and octagon also converged, effectively, to the hexagon, where the extra one or two vertex points formed only slight deviations from the hexagon or they collapsed to be effectively on top of one of the hexagon vertices. This behavior is what one would hope for in a very well-defined shape.

Similarly reassuring, when adding arcs, the hexagon emerges as a very strong shape, evidenced by those hexagon rim segments being much darker than any of the arcs over any location. Additionally, for all N tested, when N was even and the number of arcs was $N \div 2$, the strongest, most common solution converged to two straight lines roughly along the north and south rims, and arcs along the eastern and western sides. This also emerged for when N was even and the number of arcs was $\lfloor N \div 2 \rfloor$, but it was not as strong.

The difference in the area between the fitted shape and the rim trace was also an absolute minimum for the hexagon with zero arcs: Adding more sides or any arcs increased that area difference. Such a finding is a strong indicator that six sides that are straight is not only a good solution, but the best solution.

4.6. Example: Ceres' Kerwan—A Pentagon? Hexagon? Heptagon? Dodecagon?

Kerwan, the largest identified Cerean impact crater, is commonly identified as a hexagon, like Fejokoo, though Zeilnhofer and Barlow (2021b) identified it as a dodecagon. The southeastern sides, clockwise through the northwest, appear to mimic a regular hexagon's angles, and the sides appear reasonably straight. Unfortunately, as a large, degraded crater, it is significantly overprinted to the northeast, making the rim uncertain. Despite this uncertainty, we attempted to accurately trace it with the assistance of topography, using 1,711 vertex points on the 140 m/pix *Dawn* mosaic supplemented with the mean spheroid topography. The same suite of shapes as in the previous two examples were tested. We did not test up to 12 straight sides because, by eight sides, there was extremely little convergence onto a best shape.

Figure 6 shows that the southern sides are strongly linear, while the northern half of the crater is much less consistent. As with Fejokoo, when the number of arcs was $\lfloor N \div 2 \rfloor$, the shapes mostly converged to straight rim segments along the northwest and south rims, and mostly arcs along the eastern and western sides. While Kerwan and Fejokoo are only a sample size of two, this linearity along the north and south does beg the question about whether sun angle might play a role at emphasizing east and west rim variation, leading to tracing them as more straight than they actually are. Alternatively, it is possible that this preference is real and demonstrates body-wide similar stress patterns. That, however, is not part of this study, and this point is instead used to emphasize that the code works best when it has an accurate rim trace as input.

Regarding the true shape of Kerwan, Figure 6 indicates in the all-straight-edged octagon fits that the rim from the roughly 1:00 through 8:00 position tends to converge to five distinct segments. The consistency of those five edges indicates that Kerwan is likely best represented as a pentagon with those five edges and the western to northern rim represented by an arc of some sort, just not one within our constraints.

5. Discussion

In these six examples, we have shown that some are probably better fit by simple circles rather than by polygons. That does not mean a polygon cannot fit them well, though one must also be cognizant of potential biases when tracing crater rims and how lighting geometry might affect one's trace. As in the case of Copernicus, visually, an octagon fits quite well, minimizing the difference in area to a value similar to a hexagonal fit to Fejokoo. Therefore, these craters *can* be fit by these polygonal shapes, so they could be considered polygonal, and this code can be constrained to specifically find those desired solutions and objectively report their bearings and joint angles.

At issue is what was briefly addressed in the previous sections: In mathematics, one can always add terms to a fit function and converge closer to exactly representing the data. Picture, for example, 20 points in a scatter plot that very roughly form a line. They can be fit by two free parameters: a slope and y-intercept. However, they could also be fit by three free parameters in the form of a second-order polynomial (constant, x coefficient, and x^2 coefficient). One could also fit with 20 free parameters and perfectly reproduce the data. However, that high-order polynomial, in all likelihood, is not the actual function from which those data were drawn, despite perfectly representing the data. Therefore, it is considered to be "over-fit," and the lower-order fits are more likely to represent reality.

There are various ways of trying to quantify what fit is really better, and it usually is based on some combination of the residuals fit (χ^2) versus the number of free parameters (DOF). We explored two common information criteria (IC) in our search to quantify the best fit. Primarily, we focused on the Aikake Information Criterion (AIC; Akaike, 1974), which states that the better fit has the lower AIC value (which can be negative). AIC penalizes fits based on the number of free parameters, so it should be a reasonable way to determine if a nine-sided polygon really is a better fit because it is significantly better than a six-sided polygon, or if it is just a better fit because it has more free sides. In the above example, the line has DOF = 2, while the high-order polynomial has DOF = 20. The AIC's penalization of 20 versus 2, in contrast with the residuals from each solution, would indicate that the line is a better fit to the model, or more likely to represent reality.

Another common IC, the Bayesian Information Criterion (BIC; Schwarz, 1978), is identical to AIC except it penalizes differently based on DOF. Each has their adherents, and several comparisons have been published (e.g., Vrieze, 2012), but either is generally only slightly better or worse for different problems.

The purpose, then, of the IC is to provide an objective method and metric to use for model selection, assessing the quality of each model based on how good it is versus penalizing based on the number of fit parameters. So,

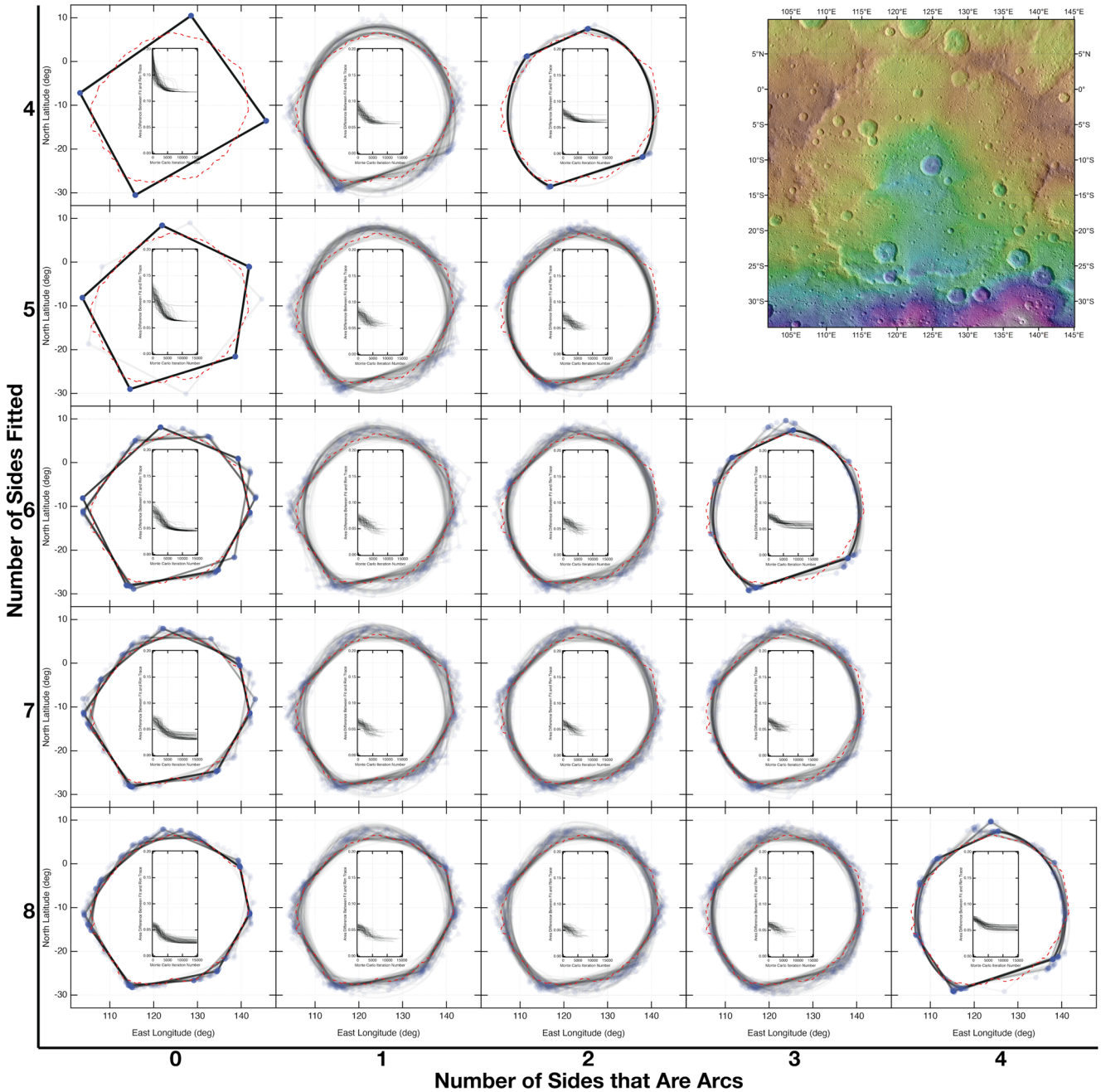

Figure 6. Same as Figure 4, except showing Kerwan crater (Ceres; 140 m/pix *Dawn* mosaic, and mean spheroid topography overlaid). Kerwan's topography is overlaid (red/brown high, purple/white low) for assistance in identifying its eroded rim; the ellipsoid has not been removed from the topography.

while Copernicus can be fit quite well by an octagon, that octagon has 16 DOF (2 *N*, the latitude and longitude of each joint), while a circle only has three DOF. Therefore, while the octagon has an area difference in the normalization of 0.025, and a circle has 0.035, the AIC for the octagon is ≈35, while for a circle it is ≈13. That lower value indicates that a circle is a better model. The same formulation strongly indicated Meteor Crater is best fit by an octagon where four sides are arcs. However, while we found that the AIC does sometimes indicate what the community would agree is the "correct" answer (e.g., the above two examples), it would similarly sometimes return picks that the community would agree are wrong. For example, no matter how many permutations of the AIC or BIC we tried, it always indicated that Fejokoo was best fit by either an octagon or a circle (depending on what version of the IC); never did it select the hexagon. Therefore, we do not include with this code a functioning version of an objective selector.

However, that does not mean an objective selector does not exist. There are additional potential methods in statistics to penalize fits based on the number of parameters, or there are potentially other likelihood functions we could use in quantifying how good the fitted shape is relative to the rim trace. For example, we are currently using a simple area difference. A different method for the likelihood could be to calculate the sum of the distances between each vertex point in the rim trace and the shape that is being tested, or their square for a more common sum-of-squares.

One could also look to completely different methods to calculate the best shape. Spectral parameters, determined by a Fourier analysis, would present an entirely different method to represent a best-fit to the rim, and such algorithms for performing the elliptical Fourier fits have been described over the last several decades (Crampton, 1995; Giardina & Kuhl, 1977; Kuhl & Giardina, 1982; Rohlf & Archie, 1984). The goal would be to add Fourier coefficients until the rim reproduced by the Fourier series captures >99% of the total cumulative power of the Fourier spectrum (or, some other defined >x%). Capturing a certain amount of the power could be one way to provide an IC to discriminate between different fits—it is effectively baked into the method itself. The above-described sum-of-squares metric could also be calculated from the output of this fitting method which could also be used to help quantify how good the fit is, though not necessarily help discriminate between different shapes and over-fitting. The issue in implementing this for our purposes is that it is not straightforward to work backwards from the best fit to understand that fit's straight versus curved rim segments and their bearings and angles, instead it could only be used to understand a minimum number of sides, which could also indicate a circle is best ("infinite" sides). Fourier analysis for understanding shapes of planetary features has been used before, such as in examining Titan's lakes (Dhingra et al., 2019).

While further explorations of these metrics will be undertaken, we think that this work alone—a code that can return the best-fit shape (once one has defined what that polygon shape is)—is still an important contribution to the field, for it is the first to attempt to objectively, algorithmically define PICs.

6. Conclusions

In this work, we have presented the output from the first attempt to objectively classify impact craters as polygonal or not, and if polygonal, what the best representation of that shape is in terms of sides and arcs. We have designed code that uses a Monte Carlo approach to this problem and we make it available to the community. We demonstrated this code on several examples of unambiguous features that "everyone" would agree are "obviously" polygonal (with caveats on the subjectivity of human classification), and we demonstrated this code on some more ambiguous examples that some literature has identified as polygonal. These different use cases are described in the online guide to using and interpreting the code, found in the code repository archives on Zenodo and GitHub.

In using this code in its present state, we recommend running it for a given crater several times to examine how frequently the same solution is found for any given n-gon shape (e.g., four-sides with one side being an arc). If the same solution is found the majority of the time, that is a strong indicator it is the true minimization for that shape. If, however, there are numerous solutions and none is strongly preferred over the others, that is a strong indicator that the crater is poorly fit by that shape, and a different one—including a circle—might be a better fit. That, in turn, would further suggest that underlying tectonics or non-uniform porosity may not exist, or if they do, have little control over that final crater shape.

Conflict of Interest

The authors declare no conflicts of interest relevant to this study.

Data Availability Statement

The code in the state described in this work is available at: https://doi.org/10.5281/zenodo.7893525. Such a repository does not allow collaborative edits nor modifications; therefore, this code may also be available at GitHub where interested parties can collaboratively edit it: https://github.com/CraterAnalysis/PolygonalCraterIdentification.

Acknowledgments
The authors acknowledge A.H. Parker for an initial version and discussions about the code, but efforts to reach A.H. Parker during preparation of this manuscript and subsequent review and publication process were not successful. The authors also acknowledge significant discussion at the 2018 meeting of the Planetary Crater Consortium held at the Southwest Research Institute in Boulder, CO, USA that motivated development of this work; in particular, C.R. Champan, J.M. Boyce, and M.F. Zeilnhofer contributed extensively to that discussion. SJR acknowledges a substantial amount of "free time" was used in the construction of this code and writing of this paper; JDR acknowledges the same. The authors acknowledge two anonymous reviewers for their helpful reviews.

References

Aittola, M., Öhman, T., Leitner, J. J., & Raitala, J. (2007). The characteristics of polygonal impact craters on Venus. *Earth, Moon, and Planets*, *101*(1–2), 41–53. https://doi.org/10.1007/s11038-007-9148-4

Aittola, M., Öhman, T., Leitner, J. J., Raitala, J., Kostama, V.-P., & Törmänen, T. (2008). The association of Venusian polygonal impact craters with surrounding tectonic structures. In *Lunar and Planetary Science Conference*. Retrieved from https://www.lpi.usra.edu/meetings/lpsc2008/pdf/2137.pdf

Akaike, H. (1974). A new look at the statistical model identification. *IEEE Transactions on Automatic Control*, *19*(6), 411526–411723. https://doi.org/10.1109/TAC.1974.1100705

Baby, N. R., Kenkamann, T., Stephan, K., & Wagner, R. J. (2023). Polygonal impact craters on Ganymede. In *Lunar and Planetary Science Conference*. The Woodlands. Retrieved from https://www.hou.usra.edu/meetings/lpsc2023/pdf/1460.pdf

Beddingfield, C. B., Beyer, R., Cartwright, R. J., Singer, K. N., Robbins, S. J., Stern, S. A., et al. (2020). Polygonal impact craters on Charon. In *Lunar and Planetary Science Conference*. The Woodlands. Retrieved from https://www.hou.usra.edu/meetings/lpsc2020/pdf/1241.pdf

Beddingfield, C. B., Burr, D. M., & Tran, L. T. (2016). Polygonal impact craters on Dione: Evidence for tectonic structures outside the wispy terrain. *Icarus*, *274*, 163–194. https://doi.org/10.1016/j.icarus.2016.03.020

Beddingfield, C. B., & Cartwright, R. J. (2020). Hidden tectonism on Miranda's Elsinore Corona revealed by polygonal impact craters. *Icarus*, *343*, 113687. https://doi.org/10.1016/j.icarus.2020.113687

Crampton, J. S. (1995). Elliptic Fourier shape analysis of fossil bivalves: Some practical considerations. *Lethaia*, *28*(2), 179–186. https://doi.org/10.1111/j.1502-3931.1995.tb01611.x

Dhingra, R. D., Barnes, J. W., Hedman, M. M., & Radebaugh, J. (2019). Using elliptical Fourier descriptor analysis (EFDA) to quantify Titan lake morphology. *The Astronomical Journal*, *158*(230), 13. https://doi.org/10.3847/1538-3881/ab4907

Dzurisin, D. (1978). The tectonic and volcanic history of Mercury as inferred from studies of scarps, ridges, troughs, and other lineaments. *Journal of Geophysical Research*, *83*(B10), 4883–4906. https://doi.org/10.1029/jb083ib10p04883

Eppler, D. T., Ehrlich, R., Nummedal, D., & Schultz, P. H. (1983). Sources of shape variation in lunar impact craters: Fourier shape analysis. *Geological Society of America Bulletin*, *94*(2), 274–291. https://doi.org/10.1130/0016-7606(1983)94<274:sosvil>2.0.co;2

Eppler, D. T., Nummedal, D., & Ehrlich, R. (1977). Fourier analysis of planimetric lunar crater shape—Possible guide to impact history and lunar geology. In D. J. Roddy, R. O. Pepin, & R. B. Merrill (Eds.), *Impact and explosion Cratering* (pp. 511–526). Pergamon Press. Retrieved from https://articles.adsabs.harvard.edu/pdf/1977iecp.symp511E

Giardina, C. R., & Kuhl, F. P. (1977). Accuracy of curve approximation by harmonically related vectors with elliptical loci. *Computer Graphics and Image Processing*, *6*(3), 277–285. https://doi.org/10.1016/S0146-664X(77)80029-4

Gou, S., Yue, Z., Ki, K., & Liu, Z. (2018). A global catalog of Ceres impact craters ≥1 km and preliminary analysis. *Icarus*, *302*, 296–307. https://doi.org/10.1016/j.icarus.2017.11.028

Hastings, W. K. (1970). Monte Carlo sampling methods using Markov chains and their applications. *Biometrika*, *57*(1), 97–109. https://doi.org/10.1093/biomet/57.1.97

Herrick, R. R. (1997). In S. W. Bougher, D. M. Hunten, & R. J. Philips (Eds.), *Morphology and morphometry of impact craters. Venus II: Geology, geophysics, atmosphere, and solar wind environment* (p. 1015). University of Arizona Press. Retrieved from https://www.lpi.usra.edu/resources/vc/vchome.shtml

Krohn, K., Jaumann, R., Wickhusen, K., Otto, K. A., Kersten, E., Stephan, K., et al. (2019). Asymmetric craters on the dwarf planet Ceres–Results of second extended mission data analysis. *Geosciences*, *9*(11), 475. https://doi.org/10.3390/geosciences9110475

Kuhl, F. P., & Giardina, C. R. (1982). Elliptic fourier features of a closed contour. *Computer Graphics and Image Processing*, *18*(3), 236–258. https://doi.org/10.1016/0146-664X(82)90034-X

Melosh, J. J., & Dzurisin, D. (1978). Mercurian global tectonics: A consequence of tidal despinning? *Icarus*, *35*(2), 227–236. https://doi.org/10.1016/0019-1035(78)90007-6

Neidhart, T., Leitner, J. J., & Firneis, M. G. (2017). Polygonal impact craters on Rhea, Dione, Tethys, Ceres, and Vesta. In *Lunar and Planetary Science Conference*. The Woodlands. Retrieved from https://www.hou.usra.edu/meetings/lpsc2017/pdf/1625.pdf

Öhman, T. (2009). The structural control of polygonal impact craters. Ph.D. Thesis. University of Oulu.

Öhman, T., Aittola, M., Korteniemi, J., Kostama, V.-P., & Raitala, J. (2010). Polygonal impact craters in the solar system: Observations and implications. Geological Society of America Special Papers. In R. L. Gibson & W. U. Reimold (Eds.), *Large meteorite impacts and planetary evolution IV* (Vol. 465, pp. 51–65). https://doi.org/10.1130/2010.2465(04)

Öhman, T., Aittola, M., Kostama, V.-P., Hyvärinen, M., & Raitala, J. (2005). Preliminary study of polygonal impact craters in Argyre region, Mars. In *Lunar and Planetary Science Conference*. Retrieved from https://www.lpi.usra.edu/meetings/lpsc2005/pdf/1731.pdf

Öhman, T., Aittola, M., Kostama, V.-P., Raitala, J., & Korteniemi, J. (2008). Polygonal impact craters in Argyre region, Mars: Implications for geology and cratering mechanics. *Meteoritics & Planetary Sciences*, *43*(10), 1605–1628. https://doi.org/10.1111/j.1945-5100.2008.tb00632.x

Öhman, T., Aittola, M., Leitner, J., & Raitala, J. (2007). Venusian polygonal impact craters. In *Lunar and Planetary Science Conference*. Retrieved from https://www.lpi.usra.edu/meetings/lpsc2007/pdf/2299.pdf

Otto, K. A., Jaumann, R., Krohn, K., Buczkowski, D. L., von der Gathen, I., Kersten, E., et al. (2016). Origin and distribution of polygonal craters on (1) Ceres. In *Lunar and Planetary Science Conference*. The Woodlands. Retrieved from https://www.hou.usra.edu/meetings/lpsc2016/pdf/1493.pdf

Otto, K. A., Jaumann, R., Krohn, K., Buczkowski, D. L., von der Gathen, I., Kersten, E., et al. (2015). Polygonal craters on dwarf-planet Ceres. In *European Planetary Science Congress*. Retrieved from https://meetingorganizer.copernicus.org/EPSC2015/EPSC2015-284.pdf

Pike, R. J. (1980). Control of crater morphology by gravity and target type: Mars, Earth, Moon. In *Lunar and Planetary Science Conference*. Johnson Space Center. Retrieved from https://articles.adsabs.harvard.edu/pdf/1980LPSC11.2159P

Robbins, S. J. (2019). A new global database of lunar impact craters >1–2 km: 1. Crater locations and sizes, comparisons with published databases, and global analysis. *Journal of Geophysical Research: Planets*, *124*(4), 871–892. https://doi.org/10.1029/2018JE005592

Robbins, S. J. (2023). *CraterAnalysis/PolygonalCraterIdentification*. Initial Public Release. [Computer Code]. https://doi.org/10.5281/zenodo.7893525

Robbins, S. J., Antonenko, I., Kirchoff, M. R., Fassett, C. I., Herrick, R. R., Singer, K., et al. (2014). The variability of crater identification among expert and community crater analysts. *Icarus*, *234*(C), 109–131. https://doi.org/10.1016/j.icarus.2014.02.022

Robbins, S. J., & Hynek, B. M. (2012). A new global database of Mars impact craters ≥1 km: 1. Database creation, properties, and parameters. *Journal of Geophysical Research*, *117*(E5), E05004. https://doi.org/10.1029/2011JE003966

Rohlf, F. J., & Archie, J. W. (1984). A comparison of Fourier methods for the description of wing shape in mosquitoes (Diptera: Culicidae). *Systematic Zoology*, *33*(3), 302–317. https://doi.org/10.2307/2413076

Schwarz, G. (1978). Estimating the dimension of a model. *Annals of Statistics*, *6*(2), 461–464. https://doi.org/10.1214/aos/1176344136

Vincenty, T. (1975). Direct and inverse solutions of geodesics on the ellipsoid with application of nested equations. *Survey Review*, *XXIII*(176), 88–93. https://doi.org/10.1179/sre.1975.23.176.88

Vrieze, S. I. (2012). Model selection and psychological theory: A discussion of the differences between the Akaike information criterion (AIC) and the Bayesian information criterion (BIC). *Psychological Methods*, *17*(2), 228–243. https://doi.org/10.1037/a0027127

Watters, W. A., & Zuber, M. T. (2007). Relating target polygonal crater morphology, tectonic setting and shallow crustal structure on Mars: A machine vision approach. In *European Geosciences Union* (Vol. 9, p. 04664). Retrieved from https://meetings.copernicus.org/www.cosis.net/abstracts/EGU2007/04664/EGU2007-J-04664-1.pdf

Watters, W. A., & Zuber, M. T. (2009). Relating target properties to the planimetric shape of simple impact craters. In *Lunar and Planetary Science Conference*. The Woodlands. Retrieved from https://www.lpi.usra.edu/meetings/lpsc2009/pdf/2556.pdf

Weihs, G. T., Leitner, J. J., & Firneis, M. G. (2015). Polygonal impact craters on Mercury. *Planetary and Space Science*, *111*, 77–82. https://doi.org/10.1016/j.pss.2015.03.014

Zeilnhofer, M. F. (2020). A global analysis of impact craters on Ceres. Ph.D. Thesis. Northern Arizona University.

Zeilnhofer, M. F., & Barlow, N. G. (2018). Preliminary investigation of the crustal characteristics of Ceres through analysis of impact craters. In *Lunar and Planetary Science Conference*. The Woodlands. Retrieved from https://www.hou.usra.edu/meetings/lpsc2018/pdf/1464.pdf

Zeilnhofer, M. F., & Barlow, N. G. (2021a). The characterization and distribution of polygonal impact craters on Ceres and their implications for the cerean crust. *Icarus*, *368*, 114586. https://doi.org/10.1016/j.icarus.2021.114586

Zeilnhofer, M. F., & Barlow, N. G. (2021b). The morphologic and morphometric characteristics of craters on Ceres and implications for the crust. *Icarus*, *368*, 114428. https://doi.org/10.1016/j.icarus.2021.114428